Stabilization System Analysis and Performance of the GEOS-A Gravity-Gradient Satellite (EXPLORER XXIX)

VINCENT L. PISACANE,* PETER P. PARDOE,† AND B. JOY HOOK‡
Applied Physics Laboratory, Silver Spring, Md.

This paper discusses the stabilization system analysis and orbital performance of the GEOS-A gravity-gradient satellite which was launched into orbit on November 6, 1965. The analysis is performed with the aid of a digital simulation of the nonlinear differential equations of motion. It includes the effects of gravity-gradient forces, orbital eccentricity, eddy current dampers, residual magnetic dipoles, solar radiation pressure, and thermal distortion of the spacecraft's stabilization boom. The attitude measuring system aboard the spacecraft is described, and processing of the attitude data is discussed. A description of the attitude determination system and a discussion of the effect of its performance on the experimental attitude results are included. Experimental attitude results are compared with the results of the digital simulation; general agreement is obtained.

Nomenclature

a	=	semi-major axis
H, H_0	=	magnitude of geomagnetic field, and value at magnetic equator
I_x, I_y, I_z	=	inertia of spacecraft about body-fixed principal axes
I_p, I_r, I_y	=	inertia of spacecraft about pitch, roll, and yaw axes
k	=	gravitational constant
M, n	=	mean anomaly and mean motion, respectively
r	=	radial distance from c.m. of earth to c.m. of spacecraft
t	=	time
β	=	sector of the orbit that is shadowed
ϵ	=	orbit eccentricity

Introduction

THIS paper discusses the design analysis and flight performance of the stabilization system of one of the Geodetic Earth Orbiting Satellites, GEOS-A. Geocentric stabilization is achieved in a passive manner by use of the gravity-gradient principle and a passive energy dissipator. The repeated success of passive gravity-gradient stabilization systems at low altitudes has fostered interest in the use of this technique for communication and meteorological satellites at higher altitudes. Since the gravity-gradient restoring torque is inversely proportional to the cube of the distance of the spacecraft from the center of the earth, it is two orders of magnitude smaller at synchronous altitudes than at low altitudes. For this reason, verification of the performance of gravity-gradient stabilization systems becomes an important consideration.

GEOS-A was conceived as part of the National Geodetic Satellite Program to study geometric and gravimetric geodesy. The following five geodetic measurement systems are employed to permit evaluation of their performance and to insure highly accurate measurements: 1) a radio Doppler system, 2) a radio ranging system, 3) a range and range rate system, 4) corner cube quartz laser reflectors, and 5) an optical beacon system. GEOS-A (Fig. 1) is the largest and most complete satellite ever constructed exclusively for the study of geodesy. It was designed and built for NASA by The Johns Hopkins University Applied Physics Laboratory (APL). Scientific and engineering direction of the project was provided by Dr. George C. Weiffenbach (the project scientist) and Ralph E. Willison (the project engineer).

For the GEOS-A mission, an earth-pointing satellite is desirable because it makes optimum use of the radiated and reflected optical and radio power. The most severe requirement of the stabilization system was imposed by the optical

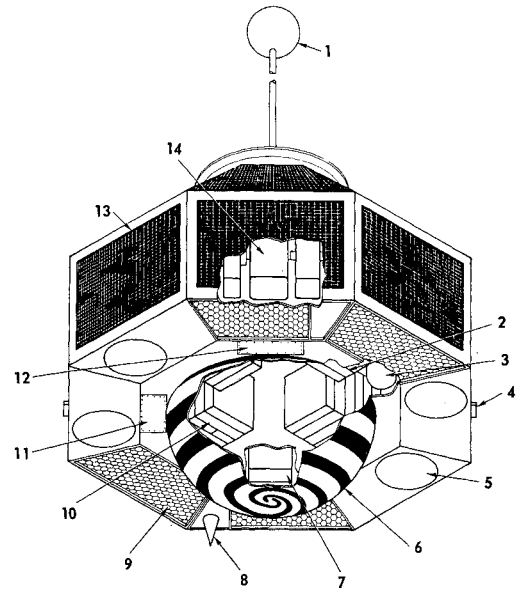

1. BOOM END MASS
2. DOPPLER TRANSMITTERS
3. DUAL OSCILLATOR
4. SOLAR ATTITUDE DETECTOR
5. OPTICAL BEACON FLASH ASSY.
6. BROADBAND SPIRAL ANTENNA
7. RANGE AND RANGE RATE TRANSPONDER
8. RANGE AND RANGE RATE ANTENNA
9. LASSER REFLECTOR PANELS
10. MEMORY
11. FLIGHT PLUG ACCESS PANEL
12. ANTENNA CONNECTOR ACCESS PANEL
13. SOLAR CELL ARRAY
14. RANGE TRANSPONDER

Fig. 1 GEOS-A spacecraft.

Presented at the AIAA/JACC Guidance and Control Conference, Seattle, Wash., August 15–17, 1966 (no paper number; published in bound volume of meeting papers); submitted August 25, 1966; revision received August 9, 1967. This work was supported by the Geophysics and Astronomy Programs Directorate of the National Aeronautics and Space Administration Headquarters. The authors are grateful to H. D. Black, M. Jennings, and M. Sturmanis for processing the experimental attitude data and for providing useful information based upon their experience with the attitude determination problem. [2.02,7.01,7.03]

* Head, Theory Project, Space Research and Analysis Group. Member AIAA.
† Associate Physicist, Space Research and Analysis Group.
‡ Senior Mathematician, Space Research and Analysis Group.

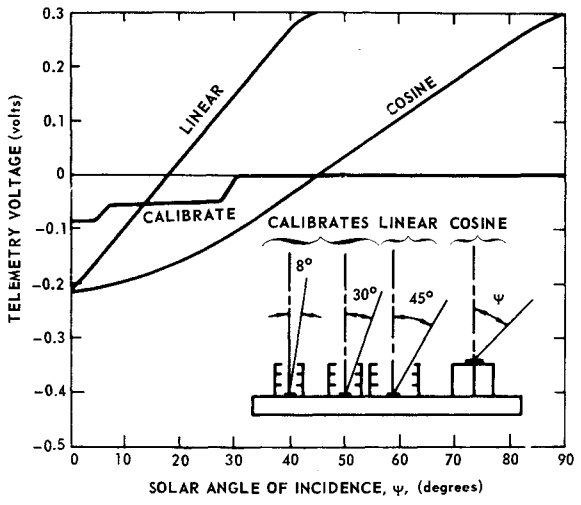

Fig. 2 GEOS-A solar attitude detector response curves.

beam pattern. This system was designed to compensate for atmospheric attenuation with large zenith angles on the assumption of achieving earth-pointing accuracy to within 5°.

Attitude Determination System

The attitude determination problem is defined mathematically as the evaluation of a transformation matrix which relates the orientation of the spacecraft to some specified reference coordinate system. The transformation matrix can be determined as a function of time if two vectors can be specified simultaneously in both the satellite and reference coordinate systems. These vector components, six scalar quantities in all, will provide redundant information for the evaluation of the three independent variables of the transformation matrix, so that in-flight calibration of the attitude system and statistical estimation of the attitude is possible. Two rather well-defined vectors which can be measured in the spacecraft with a minimum expenditure of weight and power are the unit vector of the satellite-sun line and the vector geomagnetic field. On GEOS-A, the measurement of these two vectors forms the basis of the attitude detection system.

The instrument to measure the geomagnetic field components consists of three second-harmonic-type flux-gate magnetometers. Calibration was performed at the Naval Ordnance Laboratory. In addition, partial calibration of the instrument can be achieved in-flight by superposition of known magnetic biases on the three detectors sampling the ambient magnetic field.

The satellite-sun unit vector components are measured by an array of specially designed detectors utilizing analog solar cells. After considerable study at APL, a system consisting of three types of detectors evolved.[1] Each sensor module is designed to contain the following: 1) an analog cosine sun sensor having a response grossly approximating a cosine curve as a function of the angle of incidence, 2) a detector which has a linear response in the vicinity of normal incidence, and 3) a combination of two detectors providing a step response at each of two angles in the vicinity of normal incidence (see Fig. 2).

Five solar detector modules were mounted on the GEOS-A spacecraft. One module was mounted so as to be pointing in a direction parallel to the gravity-gradient boom of the spacecraft, hereafter referred to as the $+Z$ direction, and the remaining four modules were mounted around the equator of the spacecraft pointing in mutually orthogonal directions denoted hereafter as $+X$, $-X$, $+Y$, and $-Y$. No module was mounted so as to point in the $-Z$ direction, since in the normal gravity-gradient stabilized orientation the $-Z$ axis is directed earthward. To minimize the effects of reflected light from the earth, shades were used below the equatorially mounted modules.

Experience has shown that the calibration constants for analog cosine detectors change during flight. Black has developed a program for recalibrating these instruments in flight.[2] After recalibration, attitude data are processed by the Satellite Attitude Determination Program (SAD) developed by Black and Jennings.[3] This program requires the orthogonal vector components of the earth's magnetic field vector and the orthogonal vector components of the satellite-sun unit vector, both measured in the satellite's coordinate system.

Stabilization System Description

For a satellite using gravity-gradient stabilization, initial misorientation and perturbing torques induce satellite motion about the equilibrium position, so that a damping scheme must be provided to dissipate this energy. The passive stabilization system of GEOS-A comprises a single motorized extendible boom (manufactured by the DeHavilland Company) and a General Electric magnetically anchored eddy current damper,[4] which consists of a magnet assembly at the end of the boom that is free to lock onto the magnetic field of the earth. Rotation of the magnet assembly relative to a conducting spherical shell induces eddy currents in the conductor which impedes the motion of the spacecraft. To prevent physical contact between the magnet and the conducting sphere, a diamagnetic shell of pyrolytic graphite is used as a centering device. The boom motor is controlled by ground command and backed up by an automatic stop switch activated by detents on the boom tape. This system provides bistable equilibrium about any axis normal to the local vertical. As desired for thermal uniformity, there is no preferred orientation about the longitudinal axis. A preliminary analysis indicated that this system, which would weigh approximately 11 lb, would meet the two stabilization requirements of operational status within 15 days after launch and a maximum steady-state libration amplitude of 5°. An important consideration in the selection of this system was that it had been successfully demonstrated in orbit.

Proper stabilization of the satellite can be insured if the extension of the boom is initiated when the boom axis is pointing upwards and within 55° of the local vertical. However, there was no assurance that this orientation would be obtained during a pass over the command station at APL. Another factor was that hazardous temperatures could be reached by the spacecraft, which was thermally designed to operate as a gravity-gradient satellite. Both of these considerations indicated that boom extension might need to be initiated when the boom axis is in a nonpreferred direction, possibly resulting in upside-down capture. Inversion of the spacecraft could then be accomplished by a properly timed sequence of boom retraction and extension.

Attitude Simulation

The analytical theory upon which passive gravity-gradient stabilization is based is well known. The analyses, however, tend to be complicated by the nonlinearity and coupling of the equations of motion and are intractable without simplifying assumptions about the perturbing forces. The three nonlinear differential equations for the attitude motion of a spacecraft in orbit about a gravitating mass were developed in terms of Lagragian mechanics.[5] The c.m. of the satellite is constrained to an eccentric orbit having a longitude of the ascending node and an argument of perigee that are linear functions of time. These secular variations result from the even zonal harmonics of the gravitational field, principally the J_2 term. The coupling between orbital and body motions

of the spacecraft is neglected. The attitude is expressed in terms of a set of Euler angles.

A Digital Attitude Simulator (DAS) computer program has been developed which includes the effects of gravity-gradient torques, residual dipoles, solar radiation pressure, thermal distortion of gravity-gradient booms, and passive dampers of the eddy current and hysteretic types. The integration of the nonlinear, second-order differential equations of motion over the time domain is accomplished by a fourth-order Runge-Kutta integration. The eddy-current damper is simulated on the assumption that its magnet assembly is locked to the geomagnetic field. This assumption is valid for the rather slow rates of motion of the spacecraft relative to the magnetic field and the large magnetic moments of the magnet assembly which are used. The magnitude of the damping torque is proportional to the angular velocity of the conducting shell relative to the magnet assembly. The thermal distortion of the gravity-gradient booms is handled in a quasi-static manner. Each boom is assumed to bend with a constant radius of curvature in the plane containing the undeformed boom and the sun. The boom deformation produces changes in the mass distribution parameters. The radiation pressure is computed for the booms in their undeformed position. That part of the incident radiation which is reflected is a function of the surface characteristics and is, in general, assumed to be of both the specular and diffuse types. The effects of aerodynamic torques are negligible at the altitudes of interest. A modification of the general program is used to analyze inversion maneuvers by taking into account the time-dependent mass properties of the spacecraft. It is assumed that the boom retraction and extension rates are different polynomial functions of time.

Prelaunch Design Study

Prelaunch design studies were carried out independently by APL and the General Electric Company. In general, there was very good agreement. For this particular spacecraft and orbit, the major perturbing torques arise from the gravitational, magnetic, and solar environments. The gravitational field, through the orbit eccentricity, induces a steady-state pitch libration. A linear theory in Appendix A gives an approximation to the amplitude and frequency of the perturbation. The magnetic torques arise from the interaction of the damper and residual dipole with the geomagnetic field. The coefficients used in the spherical harmonic expansion of the field constitute the Jensen-Cain model which has an rms accuracy of 9% for order 2 (8-terms) and 1% for order 4 (24-terms.[6]

Studies of the transient and steady-state performance of the spacecraft were made for the nominal orbit, which had a perigee of 600 naut miles and an apogee of 800 naut miles. The eccentric orbit, which is undesirable for accurate stabilization, is necessary for accurate satellite geodesy for which the perigee need be well defined. The nominal orbit parameters and mass properties of the spacecraft are given in Table 1. The requirement on the transient performance of the stabilization system was that the spacecraft be in operational status, that is, correctly oriented and damped to near steady-state, within 15 days after launch. This 15-day interval includes despin from about 1 to 3 rpm to near orbital rate, waiting for favorable orientation of the longitudinal axis, erection of the stabilizing boom, damping to steady-state, and, if required, the inversion maneuver and subsequent damping.

Approximations to the time constants of the despin and libration motions are possible. During the despin, the large angular velocities of the spacecraft induce rotational motion of the magnet assembly so it is not locked to the magnetic field. The simple exponential law for eddy-current damping which gives a time constant proportional to I/c is slightly optimistic. The amplitude of the libration motion after

Table 1 Satellite and orbit characteristics

Satellite characteristics in launch configuration:
I_x, I_y, I_z = 15.6, 17.4, and 20.8 slug-ft^2, respectively
M = 386.6 lbm
Satellite characteristics for 50 ft configuration:
I_x, I_y, I_z = 615.3, 617.0, and 20.8 slug-ft^2, respectively
A = 12,149 cm^2, radiation area
r = 175.3 cm, radiation moment arm
c = 70,000 dyne-cm-sec, damping coefficient
δ = 28.9 cm, thermal bending tip deflection
P_x, P_y, P_z = −56.3, 159., 250. pole-cm, dipole comp

Orbit characteristics	Actual	Nominal
Semi-major axis, km	8073.5603	7674.5410
Eccentricity	0.071922542	0.024
Inclination, deg	59.371434	59.
Ascending node, deg	40.256994	variable
Argument perigee, deg	166.75751	variable
Mean anomaly, deg	0	0
Rate of node, deg/day	−2.2457252	−2.62
Rate of perigee, deg/day	0.65242004	0.84
Time of perigee, day-year	337–1965	variable
sec	1812.4566	

boom extension depends primarily on the initial orientation of the longitudinal axis. The preferred orientation is that the boom axis is pointing up and near parallel to the local vertical. As the boom is extended, the work done by the gravitational forces will be small, so there is a tendency to conserve angular momentum. The large inertia change will reduce the rate of rotation about all axes except the longitudinal to near zero. Since the equilibrium orientation of a gravity-gradient satellite has an in-plane angular velocity of one cycle per orbital revolution, pitch librations will result. For this reason, a study of the pitch motion best illustrates the effectiveness of the damper. A linearized solution for the transient pitch libration applicable to polar and near polar orbits is given in Appendix B. The time constant of the envelope of the transient response is proportional to I_p/c, as was the despin time constant. This solution also shows that, as expected, the damper induces a disturbing torque which is inversely proportional to I_p/c. Any improvement in the transient performance by decreasing I_p/c will result in a larger disturbing torque and poorer steady-state performance. Preliminary estimates indicated that for boom lengths of 50 to 60 ft, damping coefficients of 60,000 to 80,000 dyne-cm-sec would satisfy the transient requirements. Preliminary simulation results indicated that this configuration would also satisfy the steady-state requirements. A contract was then let to the General Electric Company for the fabrication of the damper and supporting analysis.

Concurrent with the fabrication of the satellite, a detailed simulation study of the steady-state performance was initiated. For GEOS-A, the steady-state librations result principally from the orbit eccentricity, magnetic damper, residual magnetic dipole, radiation pressure, and thermal distortion of the gravity-gradient boom. It was recognized that the magnet assembly of the damper, which was not caged during launch, could induce a residual magnetic moment in the batteries which are adjacent to it. Experiments by B. Tossman of APL confirmed this and provided bounds for the magnitude of the residual magnetic moment of the spacecraft. This also meant that the magnetically anchored damper would be ineffective during the despin phase since its magnetic assembly would lock to the batteries. This problem could be circumvented by extending the boom a small distance. Once the characteristics of the damper had been fixed to a weight of 7 lb, a damping coefficient of 70,000 dyne-cm-sec, and a pole strength of 25,000 pole-cm, the remaining free variable in the steady-state analysis was the boom length. An increase in boom length, which increases the inertia of the system, tends to minimize the effects of the residual di-

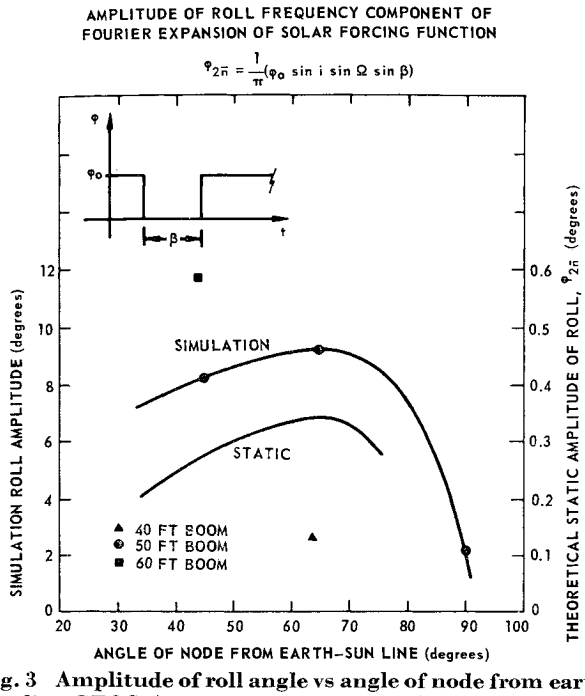

Fig. 3 Amplitude of roll angle vs angle of node from earth-sun line GEOS-A in nominal orbit and 50-ft boom length.

pole and perturbing effect of the eddy-current damper, but increases the effects of radiation pressure and thermal bending. Therefore, some optimum boom length exists which would minimize the total steady-state amplitude. Preliminary results indicated that a boom length of 50 ft would meet the 5° requirement. The boom tape was cut at 56 ft to provide a margin of 6 ft for any contingency, and a detent was made in the tape at the 50-ft length to provide automatic motor shutoff.

Subsequent analysis by the General Electric Company and APL indicated that the 50-ft length would not meet the 5° requirement over some portions of the spacecraft's lifetime. The amplitude of the solar induced libration is a function of the relative positions of the orbit and the sun. A brief analysis of the twice orbital roll component of the solar forcing function indicated that the maximum roll amplitude is a function of the angle between the earth-sun line and line of nodes and the amount of the orbit that is shadowed. The analysis indicated that for the nominal orbit, the maximum static roll amplitude induced by thermal-bending occurs when this angle is 65° and when perigee is in the shade (see Fig. 3). Digital simulation results (Fig. 3) confirmed this analytical theory and indicated that for perigee in the shadow, a maximum roll amplitude of 8.5° was possible for a 50-ft boom. Simulation results for 40-, 50-, and 60-ft boom lengths are also given in Fig. 3. These results indicated that the 40-ft boom would satisfy the steady-state requirements under the worst possible case of solar aspect and location of perigee.

Estimates of the coast time for the inversion maneuver indicated that the total time required to retract the boom, coast, and extend the boom precluded the operation during a pass over a single station. However, the maneuver could be performed over an arc of the orbit covered by two ground stations whose coverage only slightly overlapped. The NASA STADAN Station at the University of Alaska in Fairbanks together with the APL station at Howard County, Md. met this requirement.

Postlaunch Analysis

GEOS-A was launched at 1836 UT on day 310 in 1965 from the Eastern Test Range. The spacecraft was officially designated 1965 89A and titled by NASA as Explorer XXIX. Although the boost phase of the launch was normal, the second stage apparently burned to depletion. This resulted in obtaining the target perigee of 600 naut miles, but an apogee of 1230 naut miles, which is 430 naut miles higher than planned. On the first pass over Alaska, the spin rate was ~1 rpm, which confirmed the successful deployment of the despin device. No reduction in spin rate was observed during the next 14 hr., indicating that the magnetically anchored eddy-current damper was locked onto the batteries of the spacecraft.

The extension of the boom to its 3-ft detent was commanded from APL during the beginning of the 1212 universal time (UT) pass on day 311. This operation was completely successful. By observing the decay rate over several passes, a time constant of 100 min was determined. By 1900 UT on the same day the spin rate was essentially zero. After despin, the spacecraft was observed, throught elemetered-magnetometer data, to maintain a near fixed orientation with respect to the geomagnetic field. The residual magnetic dipole induced by the damper resulted in the spacecraft being near-magnetically stabilized. Reduction of the magnetometer data (by F. Mobley of APL) resulted in the direction cosines of the residual magnetic moment vector in the spacecraft's frame of reference.

As described earlier, the plan to stabilize the spacecraft was to extend the boom to 40 ft when either the boom axis achieved an orientation which would insure proper capture or the battery temperatures approached dangerous levels. On the 0805 UT pass on day 312 over APL, the battery temperatures were observed to be below the lower flight acceptance limit, so the boom was extended. The motor started at 0819 UT and stopped at 0827 UT for an elapsed time of 460 sec. This time interval corresponded to the required time for the boom to extend to about 40 ft when tested on the ground. The boom length was also inferred from telemetered data indicating the number of revolutions of a gear in the motor drive. This method indicated that the boom length was 36.8 ±1 ft. On subsequent passes, the temperature increased to nominal values, and magnetometer data confirmed that gravity-gradient capture was achieved. Unfortunately, the spacecraft was inverted. Since the solar detectors had earth shades, these earth shades now became sun shades and prevented the solar detectors from being fully illuminated. Consequently, no definitive experimental attitude data could be obtained.

At this time a simulation study of the inversion maneuver was undertaken utilizing the best estimate of the actual boom length and tracked orbit. The purpose of the study was to determine the coast time interval which would maximize the probability of success of the maneuver. Station alerts based on the tracked orbit indicated the times favorable for the two-station maneuver. A decision was made to attempt it at 1642 UT on day 317. The 5-day interval from time of gravity-gradient capture allowed most of the transient motion to be damped out. The sequence of events in the maneuver was to retract the boom to its 15-ft detent and after the coast phase to re-extend the boom. It was decided to re-extend the boom to the 50-ft detent in case a second inversion maneuver would be required. The optimum boom length could also be obtained more accurately at some future time by retraction from the 50-ft detent rather than measure the length by timing and counting gear revolutions during the inversion maneuver.

Different quadratic boom extension and retraction rates obtained from ground experiments with the GEOS-A boom were used in the simulation. The major uncertainty besides initial boom length was in the pitch librational motion at the beginning of the boom retraction phase. Since the major pitch disturbing torque arises from the orbit eccentricity, a good approximation to the pitch motion could be obtained from the linear theory given in Appendix A. The results of the simulation study are given in Fig. 4. The nominal initial conditions were computed from Eq. (A6) at the mean anomaly

corresponding to 1642 UT on day 317. Small errors in the initial pitch rate have a much greater effect on the optimum coast time than small error in pitch orientation. To study this phenomenon, runs were made in which pitch rates corresponding to pitch librations of ±3° and ±5° were added to the nominal initial conditions. A coast time of about 19.25 min was selected as that which would give the highest probability of success.

The inversion maneuver was initiated at the NASA STADAN station in Alaska and completed over the APL station. The boom retraction and extension phases took 295 and 481 sec, respectively, which compare to the ground test values of 282 and 485 sec used in the simulation. The difference in boom retraction time indicated that the boom length could have been at the upper limit of the estimated length. Surveillance of the attitude determination system during subsequent passes confirmed right-side-up capture.

A simulation study was then made to determine the performance of the spacecraft with the 50-ft boom in its actual orbit and to determine the boom length which would best meet the steady-state libration requirements. The steady-state response of the spacecraft is a function of the angle between the line of nodes and the earth-sun line, and the position of perigee. The node has a precessional rate of about 2.24 deg/day. Every 111 days the sun will have completed one revolution with respect to the orbit and there will have been four periods of increased roll libration amplitude. However, because of the increased altitude of apogee the effect of the thermal bending in roll is smaller than observed for the nominal orbit. An extrapolation indicated that the worse case occurs near day 280 in 1966 when perigee is in shade. At this time the simulation indicated that the deviation from local vertical is less than 5° about 65% of the time and reaches a peak of 7.5°. The solar effect is minimized when the sun is in the orbit plane; at this time the peak libration angle is about 5.5°. During the time of maximum solar effect, a boom length of 40 ft would result in deviations from the local vertical being under 5° about 80% of the time and a peak amplitude of 6°. Further reduction of the boom length would have little effect on the deviation from local vertical since the pitch libration dominates for the 40-ft case.

Postlaunch Attitude Detection System Performance

Although performance of the magnetometer system was satisfactory, the performance of the solar detection system

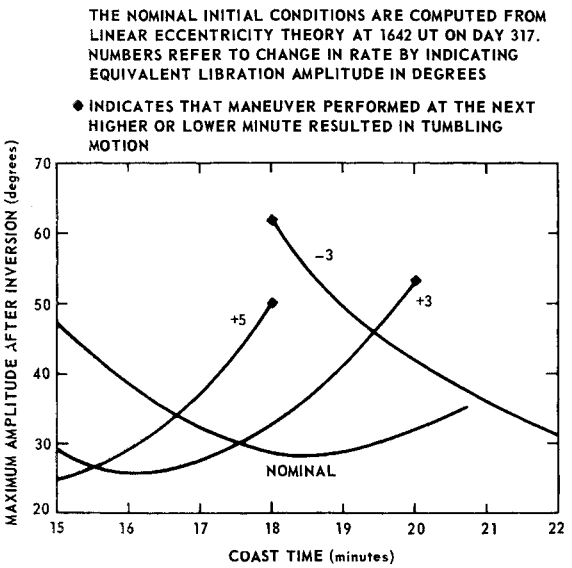

Fig. 4 GEOS-A inversion maneuver study results. Maximum amplitude after inversion as function of coast time and initial angular rate.

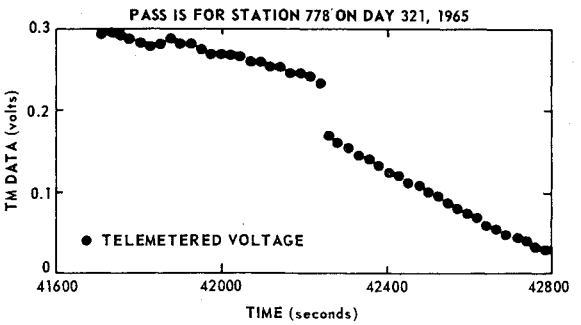

Fig. 5 GEOS-A telemetry data illustrating discontinuous response in -X cosine detector.

was disappointing. Soon after launch, data indicated that both the $+X$ and $-X$ linear detectors were not functioning. In addition, all pairs of calibration detectors exhibited a one-step response in place of the expected two-step response curve illustrated in Fig. 2. The output of the $-X$ cosine detector also exhibited an abnormal response as a function of solar angle of incidence, and the opening of a ground connection in this module on day 359 precluded the possibility of obtaining meaningful attitude data after this date.

The abnormal response of the $-X$ cosine detector is illustrated in Figs. 5 and 6. In Fig. 5 a plot of the telemetry voltage illustrates that for some passes the output was a discontinuous function of time. Abnormal response of this detector was also observed whenever the transition of illumination from the $+X$ to the $-X$ cosine detector occurred. This phenomenon, illustrated in Fig. 6 for a pass on day 329 when the sun is nearly in the plane of the orbit, produced abnormal attitude results. As illustrated by Figs. 6 and 7, the response of the Y and Z solar cosine detectors and all magnetometers indicated a continuous motion of the satellite. The rate of change of the output of the $+X$ and $-X$ cosine detectors in the vicinity of the transition region compares favorably to the orbital rate of the satellite. A lag in the response in the $-X$ cosine dector induced an apparent phase shift in the experimentally determined attitude of the sattellite, as illustrated in Fig. 8. For the portion of this pass over APL and the beginning of the pass over Santiago, where the $+X$ cosine detector is lit, good agreement is obtained between the experimental results and both the digital simulation and linear eccentricity results. For the remainder of the pass over Santiago the $-X$ cosine detector is lit, and the phase shift induced by this detector causes the difference between the experimental results and the simulation results

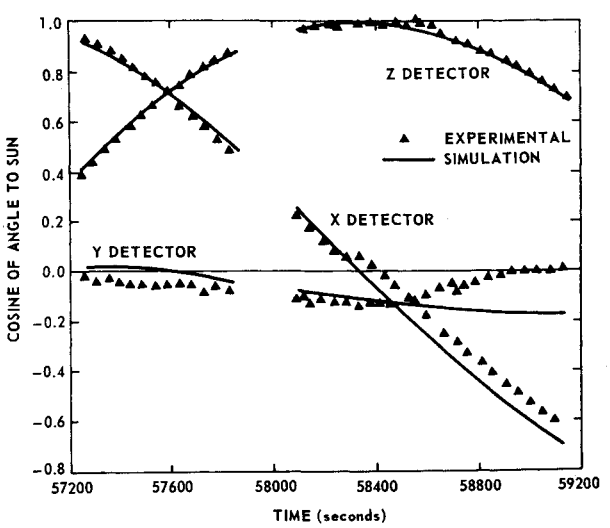

Fig. 6 GEOS-A solar cosine detector data for APL/Santiago pass on day 329.

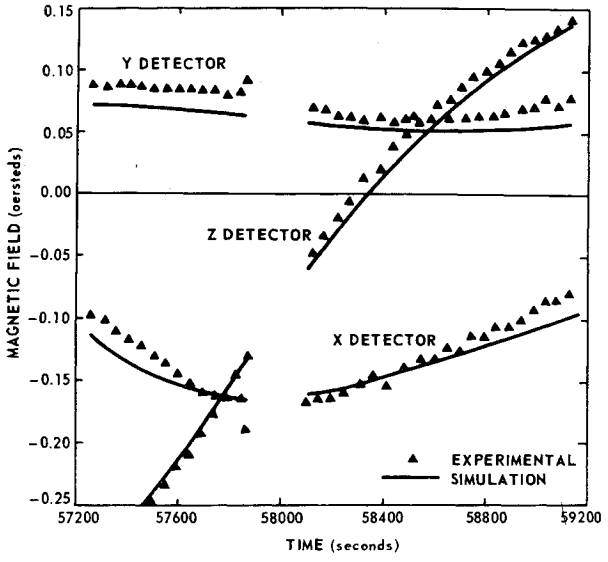

Fig. 7 GEOS-A magnetometer data for APL/Santiago pass on day 329.

to increase to approximately 7° to 8° in both pitch and roll and to nearly 5° in deviation from the local vertical. Abnormally high rates of motion are also associated with the changes in angles within this region. Statistical comparison of both portions of the pass with the digital simulation is given in Table 2. Further indication of abnormal $-X$ cosine detector performance was obtained from the magnitude of the postlaunch calibration constants. Calibration was effected from data taken in the vicinity of day 340 from four stations: Santiago, Johannesburg, Canberra, and APL. A comparison of the prelaunch with the postlaunch calibration constants is given in Table 3. A large decrease in magnitude of the calibration constants was observed for all cosine detectors with exception of the $-X$ dector. A decrease in the solar calibration constants has been observed in all other satellites built by APL. In GEOS-A, the $-X$ detector calibration constant actually increased. All of the foregoing factors support the conclusion that the $-X$ cosine detector was not functioning properly and that the attitude data based upon this detector should be disregarded.

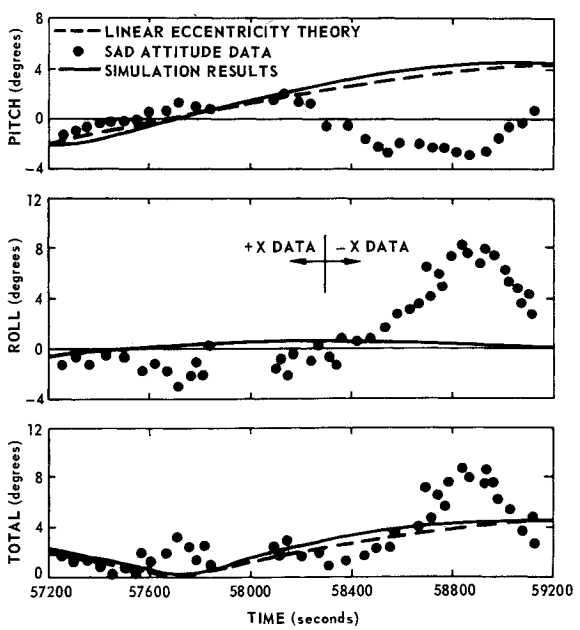

Fig. 8 GEOS-A attitude data and simulation results for APL/Santiago pass day 329.

Table 2 Statistical comparison between attitude data and simulation results for APL/Santiago Pass, day 329

	rms, deg	
	$+X$ data	$-X$ data
Pitch	0.88	5.84
Roll	1.55	4.74
Total	1.26	2.05

Comparison of Theoretical and Experimental Attitude Data

The agreement between the SAD experimental attitude and theoretical attitude of the spacecraft indicated by the simulation can be studied by examining Fig. 8, the combined APL-Santiago pass on day 329. Good agreement is obtained only over the portion of the pass during which the $+X$ solar detector is lit. The SAD experimental data, which utilize the malfunctioning $-X$ solar detector, give a physically absurd motion. An indication of the agreement between the experimental and theoretical attitude can also be inferred from a comparison of the experimental and theoretical solar and geomagnetic data (see Figs. 6 and 7). Small differences in the data over all of the double pass are observed indicating good three-axis attitude agreement. This also confirms yaw capture of the spacecraft by the geomagnetic field.

Since the Z detector data are sufficient to define the orientation of the Z axis of the satellite, the very good agreement between the Z experimental data and the simulation results should be noted. At each data point, the Z magnetometer and Z solar detector data independently define two cones of position for the Z axis of the satellite. The intersection of these two cones yields, in general, two possible orientations of the satellite's Z axis. One solution must be discarded by its indication of an abnormally large deviation from the local vertical. The results of this simplified technique are presented and compared to the simulation results in Fig. 9. The spread at each data point is the uncertainty introduced by a 1% error in the experimental magnetometer and solar data—yielding nine possible combinations of input data. In general, the results of this simplified technique indicate extreme sensitivity to small errors in input data. A comparison of the SAD determination of attitude using redundant data with the simplified technique for the APL pass indicates the necessity for redundant data. It implies an error in Z detector data in excess of 1%.

The small difference between the total deviation from local vertical as computed from the linear eccentricity theory and the simulation indicates that the effects of all other disturbing torques are small. This is because the sun is nearly in the plane of the orbit, a geometric configuration that minimizes the roll disturbance. The simulation indicates a maximum total deviation of the Z axis from the local vertical of 4.5° near the end of the Santiago pass. Results for additional passes over APL, when the $+X$ solar detector is illuminated, are given in Figs. 10 to 12 together with results of the digital simulation and the linear eccentricity theory. Similar discrepancies at the beginning of each pass are noted for pitch and roll, but there is reasonable agreement in the total deviation from local vertical when this occurs. A comparison of the experimental data over the four passes shows similarities from pass to pass indicating that a steady-state motion has been obtained and that the attitude determination system is

Table 3 Analog cosine detector calibration constants

Description of set	$+X$	$-X$	$+Y$	$-Y$	$-Z$
Prelaunch	0.437	0.360	0.492	0.508	0.444
Postlaunch	0.312	0.398	...	0.375	0.349

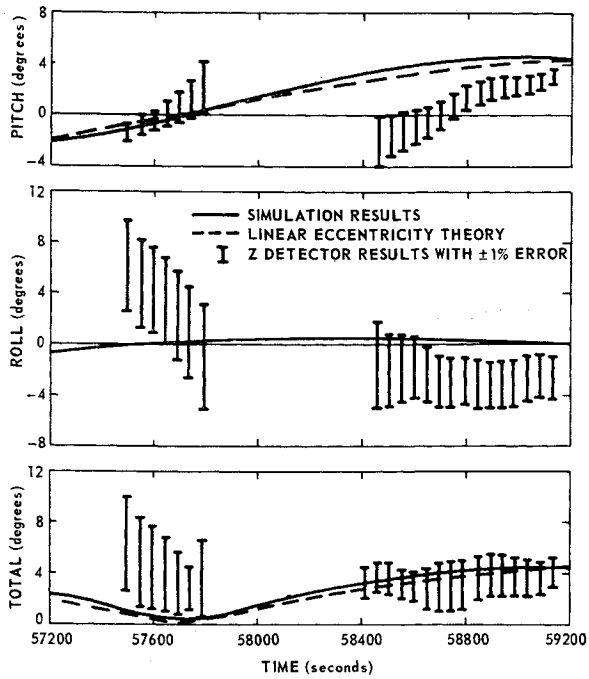

Fig. 9 Simulation and Z detector results for APL/Santiago pass day 329.

stable. A statistical comparison between the SAD experimental attitude data and the simulation results for these passes is given in Table 4.

The agreement between simulation and experimental attitude results indicates the successful performance of the GEOS-A stabilization system. The credibility of the digital simulation of the attitude motion of a gravity-gradient satellite has been supported.

Appendix A: Steady-State Libration Induced by Orbit Eccentricity

For small values of orbit eccentricity ϵ and small librational amplitudes, the pitch (in-plane) motion equation is decoupled from the roll and yaw equations; an approximate analytical solution then becomes possible. Euler's equation

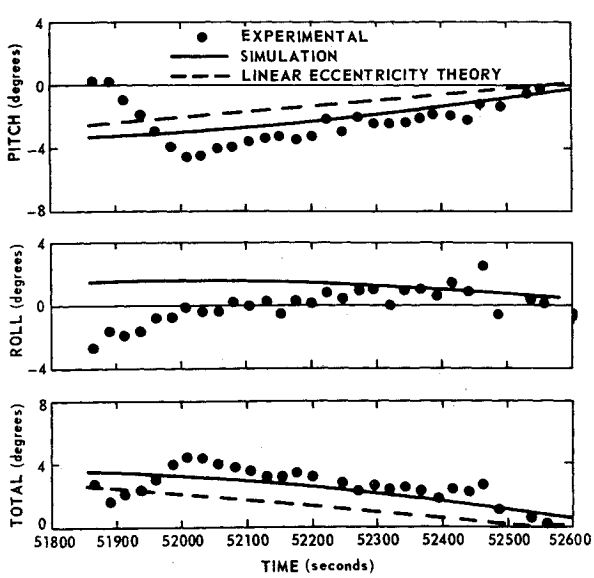

Fig. 10 GEOS-A attitude data and simulation results for APL pass on day 338.

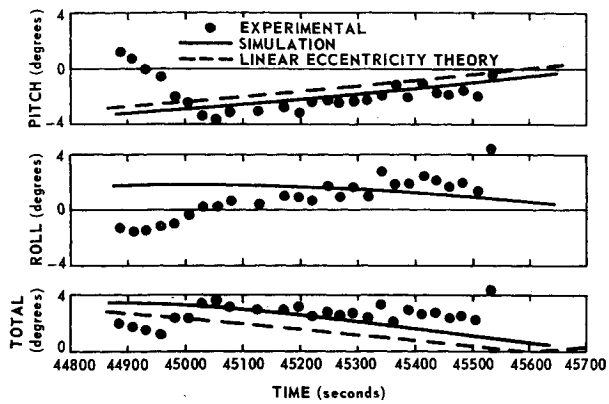

Fig. 11 GEOS-A attitude data and simulation results for APL pass on day 339.

for the pitch motion (Fig. 13), is given by

$$I_p(\ddot{\theta} + \ddot{\varphi}) = T_g = (3k/2r^3)(I_y - I_r) \sin 2\varphi \qquad \text{(A1)}$$

where T_g is the gravity-gradient torque. For an orbit of modest ϵ,

$$\theta = M + 2\epsilon \sin M + O(\epsilon^2) \qquad \text{(A2)}$$

$$r/a = 1 - \epsilon \cos M + O(\epsilon^2) \qquad \text{(A3)}$$

Substituting Eqs. (A2) and (A3) into Eq. (A1) yields

$$\varphi'' + 3\sigma\varphi = 2\epsilon \sin M + O(\varphi,\epsilon) + O(\epsilon^2) \qquad \text{(A4)}$$

where

$$M = nt \qquad n^2 = k/a^3 \qquad \text{(A5a)}$$

$$(\,)' \equiv d(\,)/dt = nd(\,)/dM = n(\,)' \qquad \text{(A5b)}$$

$$\sigma \equiv (I_r - I_y)/I_p \qquad \text{(A5c)}$$

and it has been assumed that

$$O(\varphi) = O(\epsilon) \qquad \text{(A5d)}$$

The steady-state solution to Eq. (A4) is

$$\varphi = [2\epsilon/(3\sigma - 1)] \sin M + O(\epsilon^2) + O(\varphi,\epsilon) \qquad \text{(A6)}$$

which is the induced pitch motion as a function of mean anomaly.

Appendix B: Simplified Study of the Magnetically Anchored Damper

An analysis applicable to polar and near-polar satellites yields the eddy-current damping rate and disturbing effect

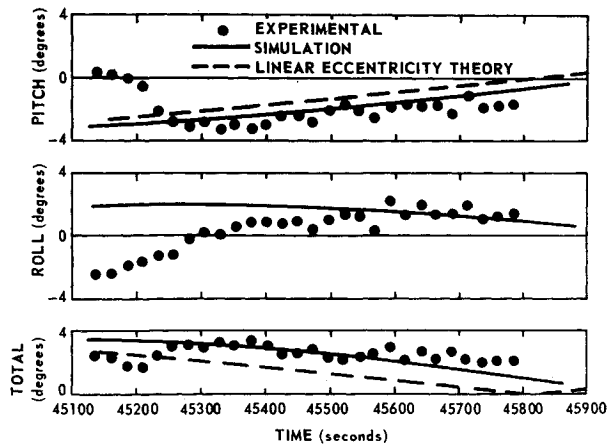

Fig. 12 GEOS-A attitude data and simulation results for APL pass on day 340.

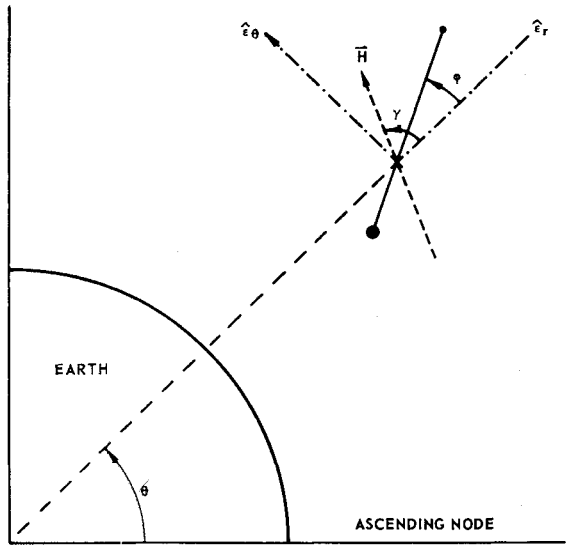

Fig. 13 In-plane configuration of spacecraft in orbit.

in terms of the damping coefficient and the inertia of the spacecraft. Extension of the gravity-gradient boom usually occurs only after the spacecraft has despun to near orbital rates. The large inertia change which accompanies boom extension reduces this rate of rotation in inertial space to near zero about all axes except the longitudinal axis. Since the satellite in its stabilized position has an angular velocity in-plane of one cycle per orbital revolution, pitch libration about this equilibrium position will result. For this reason a study of the pitch motion best characterizes the damping and perturbing effects of the damper.

The magnetic field for the satellite depicted in Fig. 13 which is assumed to move in a magnetically polar circular orbit, is given by

$$H = H_0(\cos\theta\hat{\epsilon}_\theta - 2\sin\theta\hat{\epsilon}_r) \tag{B1}$$

The angle between the local vertical and the magnetic field vector is given by

$$\gamma = -\arctan(\tfrac{1}{2}\cot\theta) \tag{B2}$$

If the magnet of the magnet assembly of the damper is collinear with the local field, the motion of the assembly relative to the conducting shell is given by

$$\dot{\gamma} - \dot{\varphi} = [2\dot{\theta}/(1 + 3\sin^2\theta)] - \dot{\varphi} \tag{B3}$$

Experiments show that the torque exerted by the magnet assembly on the conducting shell is proportional to their relative velocity, $c(\dot{\gamma} - \dot{\varphi})$; where c is the damping coefficient. For pitch motion on a circular orbit, Euler's equations of motion become

Table 4 Statistical comparison between attitude data and simulation results for APL passes on days 338, 339, and 340

	rms, deg		
	Day 338	Day 339	Day 340
Pitch	1.30	1.49	1.25
Roll	1.76	1.79	1.98
Total	0.80	1.20	0.71

$$I_p\ddot{\varphi} = T_g + T_c \tag{B4}$$

where

$$T_g \equiv (3k/2r^3)(I_y - I_r)\sin 2\varphi \qquad T_c \equiv c(\dot{\gamma} - \dot{\varphi}) \tag{B5}$$

For φ small, Eq. (B4) becomes

$$\varphi'' + \frac{c}{nI_p}\varphi' + 3\sigma\varphi = \frac{2c}{nI_p(1 + 3\sin^2\theta)} \tag{B6}$$

where

$$\sigma \equiv (I_r - I_y)/I_p \qquad (\ )' \equiv d/dM; \qquad M = nt \tag{B7}$$

The time constant, that is the time it takes for any disturbance to decrease to e^{-1} of its initial value, is given by

$$t_c = nI_p/\pi c \text{ (orbital revolutions)} \tag{B8}$$

The time constant decreases and the disturbing torque increases as the ratio c/I_p increases. This means that any improvement in transient performance by increasing c/I_p degrades the steady-state performance. These results are valid for polar and near-polar orbits. Digital simulation results indicate that Eq. (B8) is conservative.

References

[1] Fischell, R. E., "Solar cell experiments on the Transit and TRACC satellites," The Johns Hopkins University Applied Physics Lab., Rept. CM-1021 (May 1962).

[2] Black, H. D., "Attitude determination utilizing redundant sensors," *Proceedings of the IV International Aerospace Institute Symposium* (College of Aeronautics, Cranfield, England, 1966).

[3] Black, H. D., "A passive system for determining the attitude of a satellite," AIAA J. **2**, 1350–1351 (1964).

[4] Moyer, R. G., "Passive attitude control system analysis for the GEOS satellite," General Electric Spacecraft Dept., 64SD4443 (September 1965).

[5] Pisacane, V. L., Guier, W. H., and Pardoe, P. P., "Dynamical equations for the position and attitude of a spacecraft with time dependent mass and mass properties," The Johns Hopkins University Applied Physics Lab., Rept. TG-919 (June 1967).

[6] Jensen, D. C. and Cain, J. C., "An interim geomagnetic field," J. Geophys. Res. **67**, 3568–3569 (1962).